9. National Conference on Computational Mechanics
MekIT'17
B. Skallerud and H I Andersson (Eds)

IMPLEMENTATION OF NON-NEWTONIAN RHEOLOGY FOR GRANULAR FLOW SIMULATION

Petter Fornes[1,†], Hans Bihs[1] and Steinar Nordal[1]

[1]Department of Civil and Environmental Engineering
Norwegian University of Science and Technology (NTNU)
Trondheim, Norway
[†]e-mail: petter.fornes@ntnu.no

Key words: CFD, Non-Newtonian Rheology, Granular Flow, Geotechnical, REEF3D

Abstract. Landslides of the debris flow type pose a serious natural hazard. These landslides are often triggered by hydro-meteorological processes during extreme precipitation events. Debris flows usually form a dense flow composed of water and poorly graded soil particles. The propagation of these landslides greatly influences the consequences they have. The run-out of debris flows is usually simulated with depth-averaged models. These are fast to simulate due to the integration over the flow height, which reduces the problem from three to two dimensions. For the design of countermeasures resisting the pressure from the flow, it can be advantageous to use more advanced 3D numerical methods, such as computational fluid dynamics (CFD). The particle phase of debris flows has here been considered as a granular flow, and implemented as a non-Newtonian viscoplastic rheology in the open-source CFD code REEF3D. In the numerical model, the Reynolds-Averaged Navier-Stokes (RANS) equations are discretized with the fifth-order accurate Weighted Essentially Non-Oscillatory (WENO) scheme in space and with a third-order Runge-Kutta based fractional step scheme in time. The level set method used for representing the free surface handles the complex air-granular flow interface topology. The pressure gradient is modelled with Chorin's projection method for incompressible flow. The granular flow rheology includes a Coulomb frictional yield stress, increasing with the normal stress, and a viscous term that is non-linear dependent on the shear rate. The implementation has been validated using results from laboratory dam break experiments with dry sands.

1 INTRODUCTION

Debris flows and debris avalanches are landslide phenomena that can potentially cause large damages and pose a serious natural hazard [1]. A debris flow is a mix of water and poorly graded soil particles, forming a dense flow [2]. This type of landslides is often triggered by hydro-meteorological processes during extreme precipitation events, see Fig.

Figure 1: Debris flow in Hunnedalen, Norway, June 2016. [Photo: NPRA]

1. The expected increase in precipitation due to climate changes may lead to higher frequency of Norwegian debris flow events in the future. This provides the motivation for studying debris flows in the Norwegian SFI project KLIMA2050 [3], which this work is a part of.

The debris flow propagation determines a large portion of the consequences and the risk associated with the landslides. Run-out parameters include the maximum distance reached, flow velocities, thickness and distribution of deposits, as well as the interaction behavior with obstacles in the flow path [4, 5, 6]. To predict the run-out distance and to design countermeasures for reducing the consequences, a solid understanding and description of the debris flow mechanism is necessary. In engineering practice, the propagation of debris flows is usually simulated with depth-averaged models considering the debris flow as a single-phase material. These models are fast to run simulations with due to the integration over the flow height, which reduces the problem from three to two dimensions. Although neglecting variation in the velocity profile over the height reduces the accuracy of the models, they can produce sufficiently good run-out distance results. However, the complete velocity profile may be more important for interactions between the flow and structures.

For the design of countermeasures resisting the pressure from the flow, it may be necessary to use more advanced three dimensional numerical methods. With the recent increases in computer power, it is now feasible to consider methods such as Computational Fluid Dynamics (CFD). The debris flow material can also here be represented as a single-phase material, although a multiphase approach is more appropriate [7]. For the

interstitial fluid phase, consisting of water with fine particles in suspension, a viscoplastic non-Newtonian rheology may be sufficient [8]. The particle phase of debris flows can be assumed to have a non-Newtonian rheology appropriate for granular flows. In this paper, the viscoplastic Herschel-Bulkley rheology is modified to include Coulomb friction for granular flow.

2 NUMERICAL MODEL

2.1 Navier-Stokes equations

The open-source CFD code REEF3D [9] is used in this work. In REEF3D, the three-dimensional Navier-Stokes equations, which govern the behavior of viscous and incompressible fluids, are solved numerically with the finite difference method. For the conservation of mass and momentum, the code considers the continuity and Reynolds Averaged Navier-Stokes (RANS) equations:

$$\frac{\partial u_i}{\partial x_i} = 0 \tag{1}$$

$$\frac{\partial u_i}{\partial t} + u_j \frac{\partial u_i}{\partial x_j} = -\frac{1}{\rho}\frac{\partial p}{\partial x_i} + \frac{\partial}{\partial x_j}\left[(\nu + \nu_t)\left(\frac{\partial u_i}{\partial x_j} + \frac{\partial u_j}{\partial x_i}\right)\right] + g_i \tag{2}$$

where u is the velocity, ρ is the fluid density, p is the pressure, ν is the kinematic viscosity, ν_t is the eddy viscosity and g is the gravitational acceleration. On the left hand side of the RANS equations are the transient and convective velocity terms. On the right hand side are the surface and volume forces, the viscous and pressure terms, and the gravity, respectively. The Reynold stress term capturing the turbulence is modelled separately in REEF3D. However, in this paper laminar flow is considered and the eddy viscosity is set to zero.

The RANS equations are discretized in the numerical model with the fifth-order accurate Weighted Essentially Non-Oscillatory (WENO) scheme in space [10] and with a third-order Runge-Kutta based fractional step scheme in time [11].

2.2 Pressure

The pressure gradient is modelled with Chorin's projection method [12] for incompressible flow. A staggered grid is used to avoid decoupling of velocity and pressure. The momentum equation with the pressure gradient removed is solved for an intermediate velocity field u_i^*. The pressure for the new time step p^{n+1} is determined and used to correct the velocity field. In order to create divergence free flow field, the pressure needs to fulfil the following equation:

$$\frac{\partial}{\partial x_i}\left(\frac{1}{\rho\left(\phi^n\right)}\frac{\partial p^{n+1}}{\partial x_i}\right) = \frac{1}{\Delta t}\frac{\partial u_i^*}{\partial x_i} \tag{3}$$

2.3 Level set method

The level set method proposed by Osher and Sethian [13] is employed for locating the free surface. Air is modelled as a second fluid in this approach. This approach can handle the complex air-debris flow interface topology. To define the interface Γ between the two fluids, the following continuous signed distance function is used:

$$\phi(\vec{x},t)\begin{cases} >0 & \text{if } \vec{x} \in \text{phase 1} \\ =0 & \text{if } \vec{x} \in \Gamma \\ <0 & \text{if } \vec{x} \in \text{phase 2} \end{cases} \tag{4}$$

The level set function $\phi(\vec{x},t)$ is coupled to the velocity field u_j with a convection equation, and the spatial discretization is determined with the Hamilton-Jacobi WENO scheme version [14]:

$$\frac{\partial \phi}{\partial t} + u_j \frac{\partial \phi}{\partial x_j} = 0 \tag{5}$$

3 NON-NEWTONIAN RHEOLOGY

3.1 Herschel-Bulkley rheology

The non-Newtonian Herschel-Bulkley rheology has been implemented in the REEF3D CFD code [15], for the purpose of modelling the interstitial fluid phase of debris flows. The interstitial fluid consists of water with fine particles in suspension, for which the viscoplastic Herschel-Bulkley rheology can be considered appropriate [16, 17, 18].

The Herschel-Bulkley rheology has a non-linear stress relationship with the shear rate $\dot{\gamma}$ and features a yield stress τ_y. In order to have shear deformation of the material, the shear stress acting on it must exceed this yield stress. For shear stresses lower than the yield stress, the shear rate is zero. The Herschel-Bulkley rheology is defined by the following shear stress and shear rate relation:

$$\tau(\dot{\gamma}) = \tau_y + K\dot{\gamma}^n \tag{6}$$

and

$$\dot{\gamma} = \begin{cases} 0 & \text{if } \tau < \tau_y \\ \left(\frac{1}{K}(\tau - \tau_y)\right)^{\frac{1}{n}} & \text{if } \tau \geq \tau_y \end{cases} \tag{7}$$

where τ is the shear stress, $\dot{\gamma}$ is the shear rate, τ_y is the yield stress, K is the consistency parameter, n is the Herschel-Bulkley exponent. If $n > 1$ shear-thickening behavior is defined, and $n < 1$ defines shear-thinning behavior. If $n = 1$ it becomes the Bingham rheology, and if additionally $\tau_y = 0$, it becomes the Newtonian rheology.

The Herschel-Bulkley rheology is implemented in the REEF3D code as a generalized Newtonian fluid, with a non-linear shear rate dependent viscosity. The kinematic viscosity

$\nu(\dot{\gamma})$ is determined as the non-linear shear stress $\tau(\dot{\gamma})$ in Eq. 6 divided by the shear rate $\dot{\gamma}$ (and the density ρ). To prevent numerical issues related to the kinematic viscosity approaching infinity as the shear rate goes to zero, a maximum kinematic viscosity ν_0 is used for low shear rates:

$$\nu(\dot{\gamma}) = \min \begin{cases} \nu_0 \\ \left(\frac{\tau_y}{\dot{\gamma}} + K\dot{\gamma}^{n-1}\right)\frac{1}{\rho} \end{cases} \tag{8}$$

where ν is the kinematic viscosity included in Eq. 2, ν_0 is the maximum kinematic viscosity and ρ is the density. The kinematic viscosity ν is determined locally for each cell in every time step since it varies spatially and temporally, and it is considered as an isotropic property. The scalar shear rate $\dot{\gamma}$ used to calculate the viscosity is determined as the magnitude of the three-dimensional shear rate tensor $\mathbf{D}$:

$$\dot{\gamma} = \|\mathbf{D}\| = \sqrt{\frac{1}{2}\sum_{i=1}^{3}\sum_{j=1}^{3}\dot{\gamma}_{ij}\dot{\gamma}_{ij}} \tag{9}$$

The implementation of the viscosity (Eq. 8) makes the rheology bi-viscous. It results in a material that can not come to rest at a sloped angle when the flow finally slows down. Even though the viscosity is very high for low shear rates, the material will continue to flow slowly until leveling off horizontally. This is unlike depositions of landslides composed by materials with yield strength, which can support an inclined slope surface. Therefore, the flowing material will be considered as having stopped when the magnitude of velocity is several orders of magnitude lower than while propagating.

An alternative implementation to avoid infinite viscosity could be to employ a regularization parameter [19]. If so, an exponential function will be included in the yield stress term in Eq. 6, reducing it to zero for very small shear rates. This will make the shear rate dependendent viscosity function continuous, which may improve the stability. However, it will not prevent the slow deformation after depostion, and has not been considered necessary.

3.2 Granular flow rheology

Granular materials have a frictional resistance to shearing that increases with increased contact pressure between the individual particles, normally given by the Mohr-Coulomb failure criterion (Eq. 10). When granular soils are yielding, the shear stress is proportional to the effective normal stresses, which is the contact pressure between the soil grains. The internal frictional angle φ thus provides a frictional coefficient $\mu = \tan\varphi$ which determines how much shear stress the material can sustain without deforming for a given pressure. This determines for example how steep the slope angle of a pile of dry sand can be naturally.

$$\tau_y = \sigma_n' \cdot \tan\varphi + c \tag{10}$$

where τ_y is the yield shear strength, σ'_n is the effective normal stress, φ is the friction angle and c is the cohesion (low for dry granular soils).

For Eularian description of dry granular flows (or the particle phase of debris flows), modelling the granular material as a single-phase continuum, including Coulomb friction in a visco-plastic rheology can be considered. Johnson [20] proposed a Coulomb-viscous rheology for debris flows, adding the Mohr-Coulomb failure criterion (Eq. 10) as the yield strength to the Bingham rheology (Eq. 6, $n = 1$). Savage and Hutter [21] included Coulomb criterion in a depth-averaged model for dry granular flows. In the $\mu(I)$ rheology for dense granular flow by Jop et al. [22], the frictional coefficient μ is a non-linear function of the intertial number I, which is a number that depends on the shear rate and pressure. Moriguchi et al. [23] used a Coulomb-viscous rheology (Bingham with Coulomb friction for the yield strength) to back-calculate laboratory tests of dry sand dam breaks in a slope. A maximum value for the generalized viscosity was used, like in Eq. 8. Domnik et al. [24] proposed a similar Coulomb-viscoplastic model for a granular material, with a regularizition parameter included as in [25] instead of a biviscous implementation.

Here, the Herschel-Bulkley rheology (Eq. 6) is modified by including the Coulomb friction relation in Eq. 10 as the yield stress. This makes it similar to the Coulomb-viscous rheology in Moriguchi et al. [23], but also including Herschel-Bulkley exponent n makes it possible for a non-linear dependency on the shear rate. In this paper, the flowing material is assumed to be a single-phase dry sand with constant density. The effective normal stress σ'_n in the Mohr-Coulomb criterion can then be equated to the fluid pressure p (which is determined in Eq. 3 with the dry granular density). Thus, the following Coulomb Herschel-Bulkley rheology is considered:

$$\tau(\dot{\gamma}, p) = p \tan \varphi + c + K\dot{\gamma}^n \tag{11}$$

where τ is the shear stress, $\dot{\gamma}$ is the shear rate, p is the fluid pressure, φ is the dynamic friction angle of the granular material, c is cohesion, K is the consistency parameter and n is the Herschel-Bulkley exponent. This rheology is implemented in the REEF3D code like this:

$$\nu(\dot{\gamma}, p) = \min \begin{cases} \nu_0 \\ \left(\max \left[0, \frac{p \tan \varphi + c}{\dot{\gamma}} \right] + K\dot{\gamma}^{n-1} \right) \frac{1}{\rho} \end{cases} \tag{12}$$

where ν, p and $\dot{\gamma}$ are variables, determined locally in each time step, while ν_0, φ, c, ρ, K and n are material constants, given as input parameters at the start of the calculation. A max-criterion is included to ensure that the expression for the yield stress is never lower than zero, which could make the viscosity negative. That is unphysical and would also cause severe convergence problems.

For a dry sand with only compressible air in the pore spaces, the assumption $\sigma'_n = p$ is considered acceptable. For a debris flow however, the presence of interstitial pore water fluid, may complicate the situation. If considering both the water fluid phase and

the granular particle phase, an Eularian multiphase (mixture theory) approach might be suitable [26, 27]. It has been observed that interstitial pore water fluid pressure can build up during deformation, which reduces the contact stress between the particles and consequently reduces the frictional resistance of the flowing mass [28]. When there is water present, the effective normal stress can be determined as the total normal stress (pressure) minus the interstitial pore fluid pressure. The build up of so-called excess pore pressure should be considered in the rheology.

4 EXPERIMENTS

To validate the REEF3D Coulomb frictional yield stress implementation, a laboratory dam break test with dry sand by Moriguchi et al. [23] is considered here. $50kg$ of the material was placed in a box 50x30x30cm. It was released and driven only by gravity down a 180cm long, 30cm wide flume, with slope angles $\theta = 45, 50, 55, 60, 65°$. At the end of the slope, a plate with a pressure sensor measured the impact force.

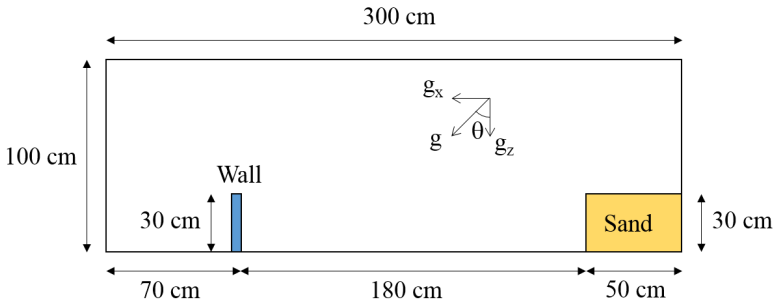

Figure 2: Model experiment dimensions

Simulation of this experiment has been done with a 2D REEF3D model (1 cell out of the plane), see Fig. 2. The calculation domain had dimensions 300x100cm and cell length was 0.25cm. This resulted in a mesh with 480000 cells. A 30cm tall, 5cm wide obstacle was placed 180cm from the 50x30cm starting sand body, representing the pressure plate. The rest of the domain was filled with air, with density $1.205kg/m^3$ and kinematic viscosity $1.41 \cdot 10^{-5}m^2/s$. The experiment simulated here was done with a slope angle θ of 45°. In the numerical model, this was modelled by giving the gravitational acceleration as $g_x = g \cdot \sin\theta$ and $g_z = g \cdot \cos\theta$.

The material properties in the numerical simulation are presenteted in Table 1. These base case values were based on the values used by Moriguchi et al. [23]. A parametric study was done to check the senstivity of the material properties included in Coulomb Herschel-Bulkley rheology; friction angle φ, cohesion c, consistency parameter K and the Herschel-Bulkley exponent n. The parameters were varied individually, values are presented in Table 2. One case was added where the friction angle was set to zero, which

means that the yield strength is equal to the cohesion. This makes it essentially the Herschel-Bulkley or Bingham ($n = 1$) rheology, without the Coulomb friction.

Table 1: Base case material properties

Material property	Unit	Base case
Density ρ	$[kg/m^3]$	1379.0
Maximum kinematic viscosity ν_0	$[m^2/s]$	1000000.0
Friction angle φ	$[^\circ]$	30.0
Cohesion c	$[Pa]$	1.0*
Consistency parameter K	$[Pa \cdot s^n]$	1.0
Herschel-Bulkley exponent n	$[-]$	1.0

*Small value assumed to avoid numerical issues

Table 2: Parametric study of material properties, parameters sets (PS)

Parameter	Unit	PS-BC	PS-φ	PS-c	PS-K	PS-n	PS-τ_y
φ	$[^\circ]$	30.0	45.0	30.0	30.0	30.0	0.0
c	$[Pa]$	1.0	1.0	1000.0	1.0	1.0	1000.0
K	$[Pa \cdot s^n]$	1.0	1.0	1.0	10.0	1.0	1.0
n	$[-]$	1.0	1.0	1.0	1.0	0.35	1.0

5 RESULTS

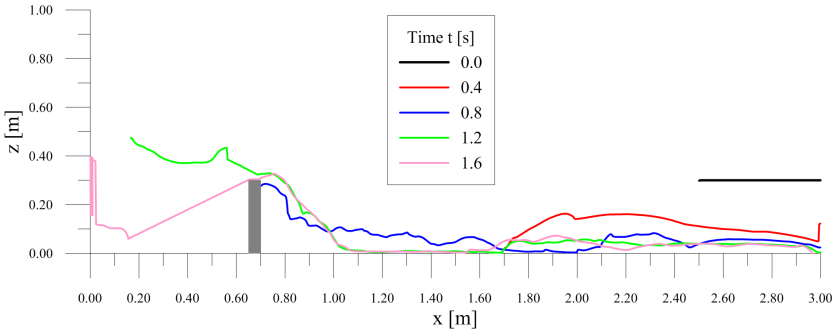

Figure 3: Base case, free surface elevation with time t [s]

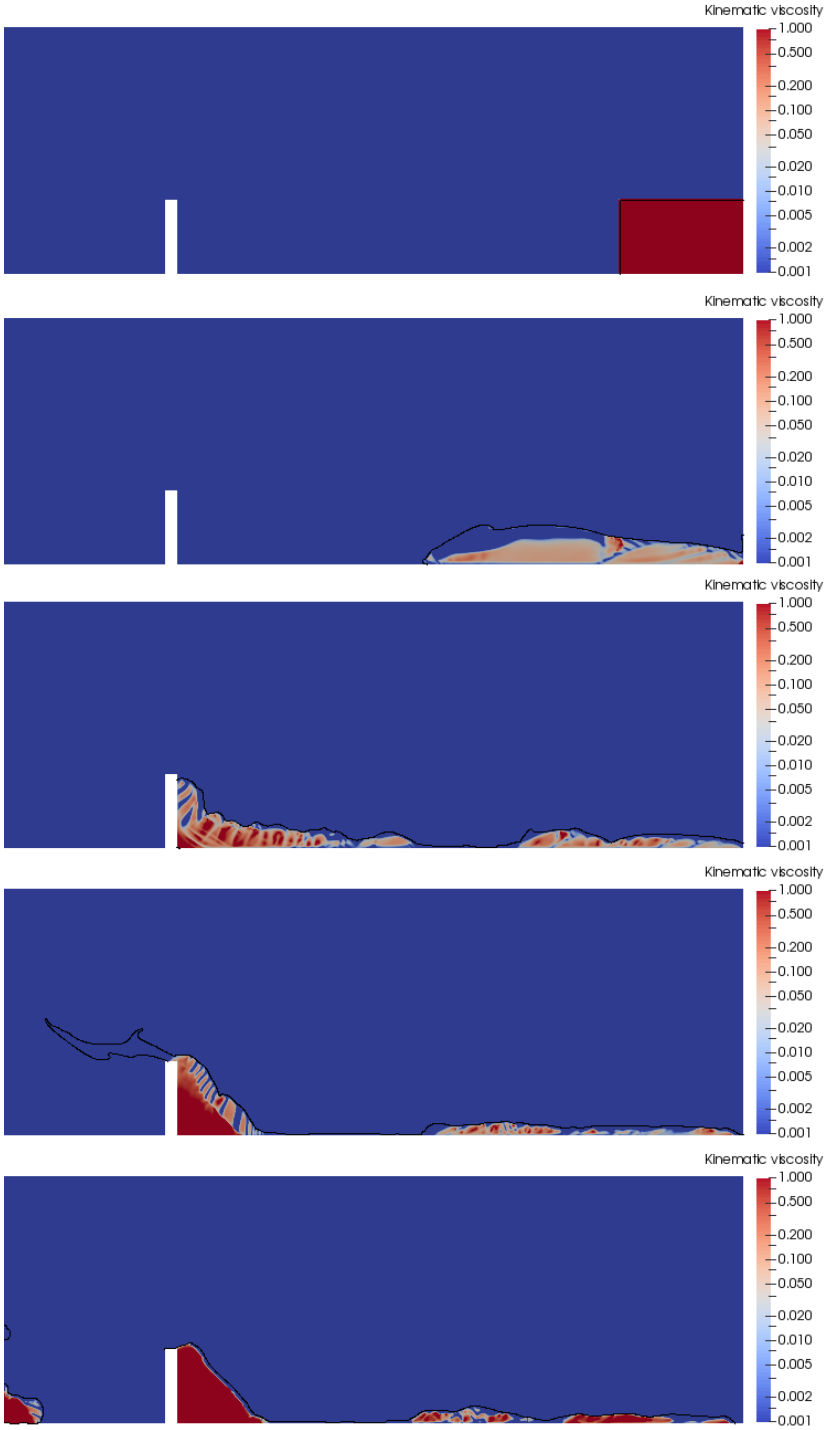

Figure 4: Base case, kinematic viscosity ν at time $t = 0.0, 0.4, 0.8, 1.2, 1.6s$

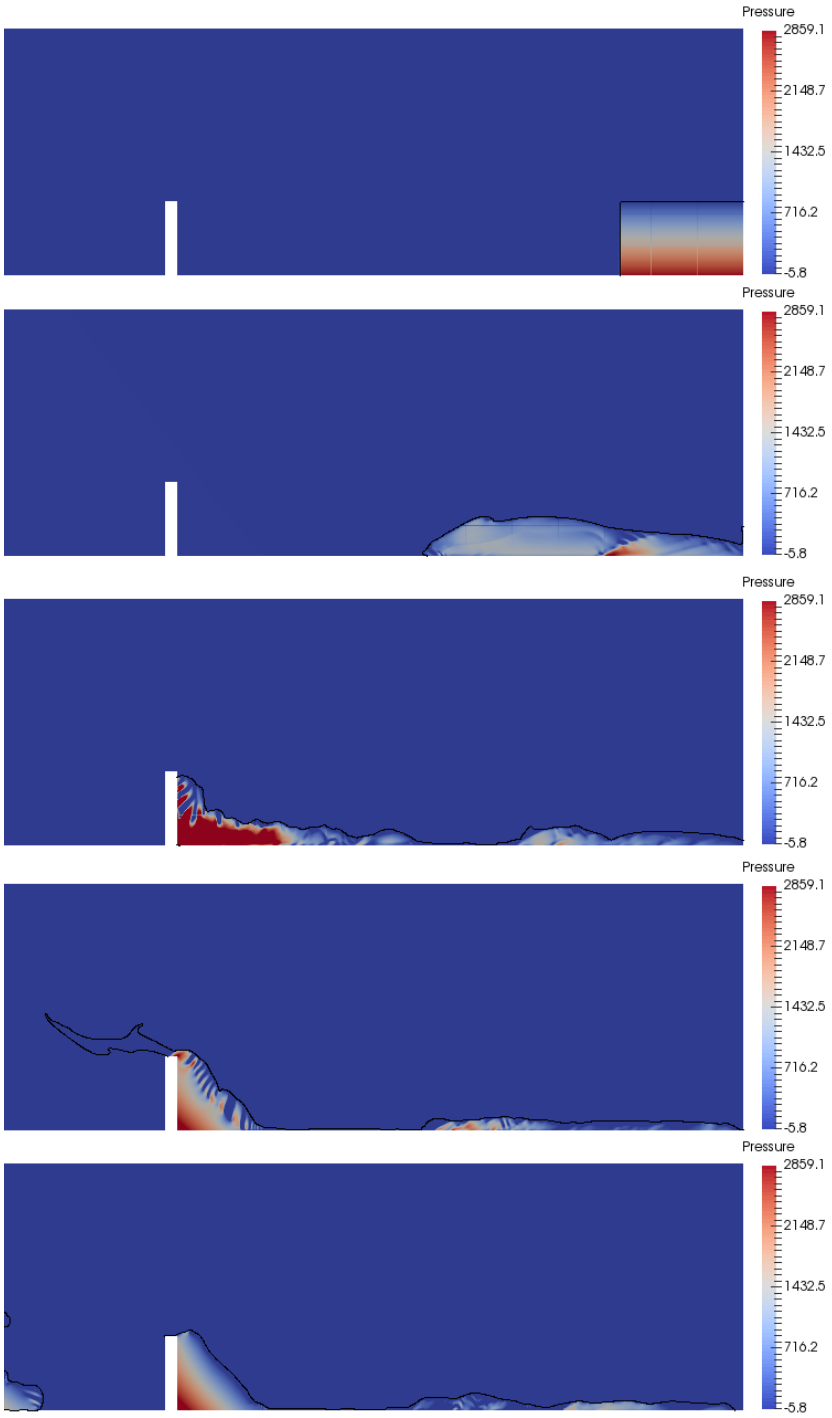

Figure 5: Base case, pressure p at time $t = 0.0, 0.4, 0.8, 1.2, 1.6s$

The results from the numerical simulations of the dam break experiments are presented

here. Fig. 3 shows the evolution of the free surface with time for the base case material properties given in Table 1. After around $0.8s$ the sand starts to flow over the wall, which was not included in the physical experiment. Compared to the experimental results in [23], the main flow behaviors observed in the laboratory was captured in the numerical simulation.

Fig. 4 shows contours of the kinematic viscosity ν, which depends on the local shear rate $\dot{\gamma}$ and the local cell pressure p. The pressure is shown in Fig. 5. Shear bands can be observed where the viscosity is low due to the locally high shear rates. Because of the coupling between pressure and velocity, this affects the pressure contours.

The pressure acting on the wall obstructing the flow is integrated, and the total horizontal forces with time is presented in Fig. 6. The figure also shows the results from the sensitivity study of the different material properties. For both cases with increased cohesion, there are large oscillations after the impact. There seems to be less spikes in the force at impact and more gradual increase when either friction angle or consistency parameter is increased. The final forces reached in all the cases have similar values as in

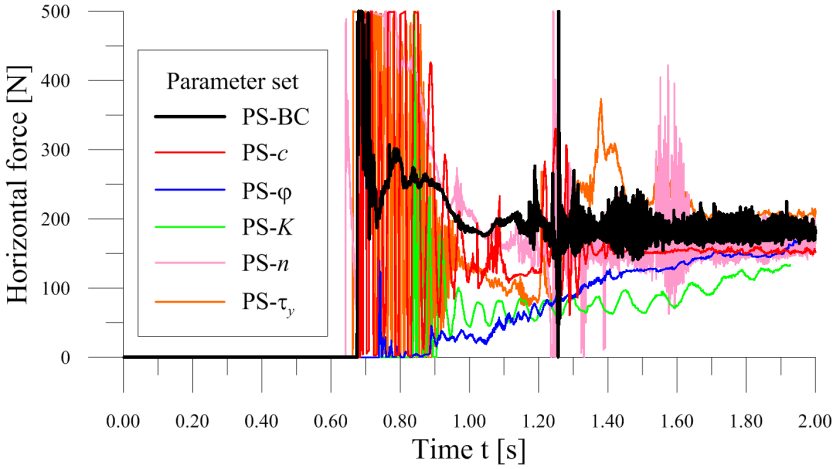

Figure 6: Horizontal forces acting on wall with time (spikes cropped at 500 N)

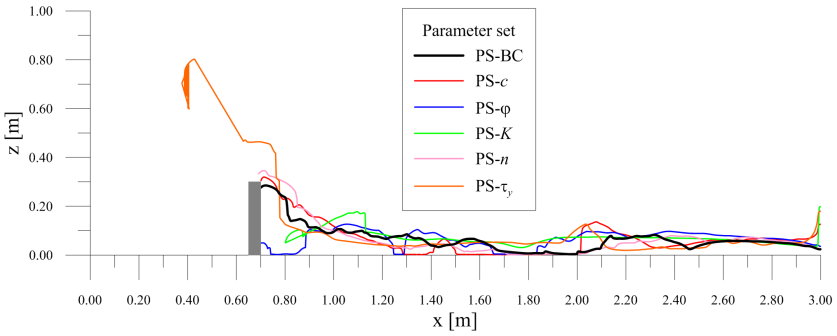

Figure 7: Parametric study, free surface elevation at time $t = 0.8s$

the original experiment, almost $200N$. There, the same extent of oscillations and spikes were not observed, however.

The effect of the individual material properties is also shown in Fig. 7, plotting the free surfaces at time $t = 0.8s$. There is little effect observed of varying the Herschel-Bulkley exponent n from 1.0 to 0.35. The latter value is appropriate for fine grain suspensions [8]. Increasing consistency parameter K increases the viscous shear stress, and increasing the friction angle φ increases the contribution from the Coulomb friction to the yield strength. For both cases, the flow is slowed slightly down, and impacts the wall later. Increasing the cohesion c also increases yield strength, but does not affect the results at $0.8s$ much. Only using increased c, with zero friction angle, makes the flow quite more mobile. Back-calculation has not been done to obtain a parameter set with better match to the experimental results. To improve the match, a higher friction angle and consistency parameter should be considered.

6 CONCLUSIONS

- A non-Newtonian granular flow rheology is implemented in the REEF3D open-source CFD code. Coulomb frictional yield stress is included in the viscoplastic Herschel-Bulkley rheology. It has been validated for laboratory dam break experiments on dry granular sand.

- The yield stress is modelled as a very high viscosity at low shear rates with the generalized Newtonian implementation. This means that even if a flowing material slows down and is practically depositioned, the deformation will never stop until resting with a horizontally levelled surface. This can be considered sufficent as long as the velocity becomes very small. To allow for deposition with a sloped surface the yield stress should be accounted for more realistically, potentially with a coupled elastoplastic and viscoplastic model.

- The implemented rheology can be appropriate for the particle phase of debris flows. However, full debris flow behavior, including the collisions between the larger sized grains, the buildup of excess pore pressure, temporal and spatial rheological changes, cannot realistically be captured with a single-phase continuum material. An Eularian multiphase CFD model may be suitable for this purpose.

REFERENCES

[1] Takahashi, T. *Debris flows: mechanics, predictions and countermeasures* (2007) Taylor & Francis, New York

[2] Iverson, R.M. The physics of debris flows. *Reviews of Geophysics* (1997) 35(3):245-296.

[3] KLIMA2050, *www.klima2050.no*

[4] Crosta, G.B., Cucchiaro, S. and Frattini, P. Validation of semi-empirical relationships for the definition of debris-flow behavior in granular materials. *Debris-Flow Hazards Mitigation: Mechanics, Prediction, and Assessment, Vols 1 and 2* (2003) 821-831.

[5] Rickenmann, D. Runout prediction methods. *Debris-flow hazards and related phenomena* (2005) Springer, 305-324.

[6] Hungr, O. Classification and terminology. *Debris-flow hazards and related phenomena* (2005) Springer, 9-23.

[7] Iverson, R.M. The debris-flow rheology myth. *Debris-Flow Hazards Mitigation: Mechanics, Prediction, and Assessment, Vols 1 and 2:* (2003) 303-314.

[8] Laigle, D. and Coussot, P. Numerical modeling of mudflows *Journal of Hydraulic Engineering-Asce* (1997) 123(7):617-623.

[9] Bihs, H., Kamath, A., Alagan Chella, M., Aggarwal, A. and Arntsen, .A. A new level set numerical wave tank with improved density interpolation for complex wave hydrodynamics. *Computers & Fluids* (2016) 140:191-208.

[10] Jiang, G.S. and Shu, C. W. Efficient implementation of weighted ENO schemes. *Journal of Computational Physics* (1996) 126(1):202-228.

[11] Shu, C.W. and Osher, S. Efficient Implementation of Essentially Non-Oscillatory Shock-Capturing Schemes. *Journal of Computational Physics* (1988) 77(2):439-471

[12] Chorin, A.J. Numerical Solution of Navier-Stokes Equations. *Mathematics of Computation* (1968) 22(104): 745-&.

[13] Osher, S. and Sethian, J.A. Fronts Propagating with Curvature-Dependent Speed - Algorithms Based on Hamilton-Jacobi Formulations. *Journal of Computational Physics* (1988) 79(1):12-49.

[14] Jiang, G.S. and Peng, D.P. Weighted ENO schemes for Hamilton-Jacobi equations. *Siam Journal on Scientific Computing* (2000) 21(6):2126-2143.

[15] Fornes, P., Bihs, H., Thakur, V. and Nordal, S. Implementation of non-Newtonian rheology for debris flow simulation with REEF3D. *Proceedings of the 37th IAHR World Congress*(Submitted)

[16] Coussot, P., Laigle, D., Arattano, M., Deganutti, A. and Marchi, L. Direct determination of rheological characteristics of debris flow. *Journal of Hydraulic Engineering-Asce* (1998) 124(8):865-868.

[17] Kaitna, R. and Rickenmann, D. Flow of different material mixtures in a rotating drum. *Debris-Flow Hazards Mitigation: Mechanics, Prediction, and Assessment. Proceedings of the 4th International DFHM Conference, Chengdu, China, Citeseer.* (2007)

[18] Kaitna, R., Rickenmann, D. and Schatzmann, M. Experimental study on rheologic behaviour of debris flow material. *Acta Geotechnica* (2007) 2(2):71-85.

[19] Saramito, P. and Wachs, A. Progress in numerical simulation of yield stress fluid flows. *Rheologica Acta* (2016) :1-20.

[20] Johnson, A.M. *Physical processes in geology: A method for interpretation of natural phenomena; intrusions in igneous rocks, fractures, and folds, flow of debris and ice* (1970) Freeman, Cooper.

[21] Savage, S.B. and Hutter, K. The motion of a finite mass of granular material down a rough incline. *Journal of Fluid Mechanics* (1989) 199:177-215.

[22] Jop, P., Forterre, Y. and Pouliquen, O. A constitutive law for dense granular flows *Nature* (2006) 441(7094):727-730.

[23] Moriguchi, S., Borja, R.I., Yashima, A. and Sawada, K. Estimating the impact force generated by granular flow on a rigid obstruction. *Acta Geotechnica* (2009) 4(1):57-71.

[24] Domnik, B., Pudasaini, S.P., Katzenbach, R. and Miller, S.A. Coupling of full two-dimensional and depth-averaged models for granular flows *Journal of Non-Newtonian Fluid Mechanics* (2013) 201:56-58.

[25] Papanastasiou, T.C. Flows of Materials with Yield *Journal of Rheology* (1987) 31(5):385-404.

[26] Iverson, R.M. and George, D.L. A depth-averaged debris-flow model that includes the effects of evolving dilatancy. I. Physical basis. *Proceedings of the Royal Society a-Mathematical Physical and Engineering Sciences*(2014) 470(2170).

[27] von Boetticher, A., Turowski, J.M., McArdell, B.W., Rickenmann, D. and Kirchner, J.W. DebrisInterMixing-2.3: a Finite Volume solver for three dimensional debris flow simulations based on a single calibration parameter-Part 1: Model description. *Geoscientific model development discussions* (2016) 8(8).

[28] McArdell, B.W., Bartelt, P. and Kowalski, J. Field observations of basal forces and fluid pore pressure in a debris flow. *Geophysical Research Letters* (2007) 34(7)